Shear-induced dispersion in a dilute suspension of rough spheres

By F. R. DA CUNHA† AND E. J. HINCH

Department of Applied Mathematics and Theoretical Physics, The University of Cambridge, Silver Street, Cambridge CB3 9EW, UK

In the absence of Brownian motion, inertia and inter-particle forces, two smooth spheres collide in a simple shear flow in a reversible way returning to their initial streamlines. Because the minimum separation during the collision can be less than 10^{-4} of the radius, quite a small surface roughness can have a significant irreversible effect on the collision. We calculate the change between the initial and final streamlines caused by roughness. Repeated random collisions in a dilute suspension lead to a diffusion of the particles across the streamlines. We calculate the shear-induced diffusivity for both self-diffusion and down-gradient diffusion.

1. Introduction

Shear-induced dispersion is important in mixing particles across streamlines of pipe and channel flows. Eckstein, Bailey & Shapiro (1977) noted that mixing is needed in blood flow to produce a diffusional flux of platelets to a thrombus on a wall, and also to transport oxygen-saturated red cells to unsaturated regions. Mixing can also counter systematic migration of particles in rheometry (Leighton & Acrivos 1987*b*) and is useful in the resuspension of a sediment.

The first experimental investigation of shear-induced migration was made by Eckstein *et al.* (1977) who monitored the random walk of a radioactively marked particle in the gap of a Couette device. For particles of size a in a flow of shear rate γ, they found at moderate concentrations a self-diffusivity of the random walk across the streamlines D which was proportional to γa^2, with a numerical coefficient of order 0.025. At low volume fractions $\phi < 0.2$, they found that the diffusivity was approximately linear in the concentration of the suspension. Leighton & Acrivos (1987*a*) used the time to circulate the Couette device to obtain more precisely the position across the flow, finding $D \approx 0.5\phi^2\gamma a^2$ for $0.05 < \phi < 0.4$.

Numerical simulations have been made by Bossis & Brady (1987) for spheres in a monolayer using their Stokesian dynamics. They found that when Brownian motion is small the cross-stream diffusivity scales with γa^2, with a numerical coefficient of 0.074 at an areal fraction of $\phi_A = 0.453$.

Because two smooth spheres return to their original streamlines after a collision, theoretical studies are complicated even in dilute suspensions by the necessity of considering more than two particles. Recently Wang, Mauri & Acrivos (1995) have examined three spheres interacting in a certain approximation, finding a cross-stream

diffusivity of $0.11\phi^2\gamma a^2$. Earlier Acrivos *et al.* (1992) had calculated the dispersion along, rather than across, the streamlines, which involved a far-field interaction between four spheres as two pairs.

When two spheres collide in a shear flow, the minimum separation can be less than 10^{-4} of their radius. A small surface roughness can therefore have a large effect. Now Smart & Leighton (1989) observed that a sample of $43\,\mu\text{m}$ glass spheres had surface asperities of the order of $0.4\,\mu\text{m}$, and that these stopped the spheres becoming closer than the asperities. Arp & Mason (1977) showed that a small surface roughness could eliminate the closed doublets in which two close spheres circle one another indefinitely in shear flow. In this paper we explore the effect of surface roughness on the collisions between two spheres. We will suppose that the asperities exert a normal force between the surfaces of two spheres which resists their becoming closer than the asperities but which does not exert any resistance as they separate. (We will also need to make assumptions about the tangential component of the contact force.) The difference between approach and separation makes the collision irreversible, so that the particles separate on streamlines further apart than on their approach. There is thus a migration of particles across streamlines, and this leads to a shear-induced dispersion. A similar random migration of a rough heavy sphere sedimenting through a suspension of neutrally buoyant sphere has been studied by Davis (1992).

2. Particle trajectories

2.1. *Governing equations*

We consider a dilute suspension of small rigid non-colloidal spheres of radius a, which are immersed in a viscous fluid undergoing a simple shear flow

$$\boldsymbol{u} = (\gamma y, 0, 0)\,.$$

We suppose that the spheres are sufficiently small for inertial forces to be negligible in the particles and in the fluid. On the other hand we suppose that the spheres are sufficiently large for Brownian and other physico-chemical interactions to be negligible. Finally we assume that the particles are neutrally buoyant. Under these conditions, the hydrodynamic forces and couples on the particles must vanish, with the viscous flow being obtained from solving the Stokes equations.

In a dilute suspension we need only consider in detail the interaction between two spheres. Let the centres of the two spheres be $X(t)$ and $Y(t)$. Now the centre of mass of two equal spheres translates with the simple shear, i.e.

$$\dot{X}_1(t) + \dot{Y}_1(t) = \gamma\left(X_2^{-\infty} + Y_2^{-\infty}\right),$$
$$X_2(t) + Y_2(t) = X_2^{-\infty} + Y_2^{-\infty},$$
and $\qquad X_3(t) + Y_3(t) = X_3^{-\infty} + Y_3^{-\infty},$

where the superscript denotes the value far upstream at $t = -\infty$. The relative motion $x(t) = X(t) - Y(t)$ is described by Batchelor & Green (1972a). Non-dimensionalizing lengths with the radius of the spheres a and times with the inverse shear rate $1/\gamma$, they give

$$\dot{x} = y + ex - \tfrac{1}{2}By\,,$$
$$\dot{y} = \quad ey - \tfrac{1}{2}Bx\,,$$
$$\dot{z} = \quad ez\,,$$

where
$$e = xy(B - A)/r^2 \quad \text{and} \quad r^2 = x^2 + y^2 + z^2 .$$
Here $A(r)$ and $B(r)$ are mobility functions for the motion parallel and perpendicular to the line of centres.

2.2. *Mobility functions*

Expressions for the mobility functions $A(r)$ and $B(r)$ can be found in Tables 11.23–27 of the book by Kim & Karrila (1991). In the far field $r \geqslant 2.5$, we use the forms
$$A = 5r^{-3} - 8r^{-5} + 25r^{-6} - 35r^{-8} + 125r^{-9} - 102r^{-10} + 12.5r^{-11} + 430r^{-12} ,$$
$$B = \tfrac{1}{3}\left(16r^{-5} + 10r^{-8} - 36r^{-10} - 25r^{-11} - 36r^{-12}\right) .$$
In the lubrication region $2 < r \leqslant 2.01$, we use
$$A = (16.3096 - 7.1548r)/r ,$$
$$B = 2\left(0.4056L^2 + 1.49681L - 1.9108\right)/r\left(L^2 + 6.04250L + 6.32549\right) ,$$
where $L = -\ln(r - 2)$. In the intermediate region $2.01 < r < 2.5$, we use a least-squared-fit of a fifth-order polynomial in r^{-1} to the data of Lin, Lee & Sather (1970)
$$A = -4.3833 + 17.7176r^{-1} + 14.8204r^{-2} - 92.4471r^{-3} - 46.3151r^{-4} + 232.2304r^{-5} ,$$
$$B = -3.1918 + 12.3641r^{-1} + 11.4615r^{-2} - 65.2926r^{-3} - 36.4909r^{-4} + 154.8074r^{-5} .$$

This fit is within 3% of the data in the range $2.01 < r < 2.5$.

2.3. *Model of roughness*

The electron micrographs of Smart & Leighton (1989) showed spheres covered with isolated asperities of the size of 10^{-3} to 10^{-2} of a particle radius. Apparently the process of manufacture generates small debris which becomes attached to the otherwise smooth spheres. The density of these asperities was sufficiently large to prevent the smooth parts of the surfaces coming into contact: always a smooth surface would contact an asperity. On the other hand the density of the asperities was sufficiently sparse not to interfere with the lubrication between the two surfaces. Other types of particles may be different.

Let the non-dimensional minimum separation between the surfaces of the two spheres be ϵ. In reality this will vary between different spheres and even between different contacts of the same spheres. We shall assume, however, that all contacts have the same minimum separation $r = 2 + \epsilon$ between the centres of the spheres.

As described in the introduction, we model the effect of the roughness by assuming that, when the particles are at their minimum separation, a normal force is exerted to stop the particles becoming closer, but no force is exerted when the particles separate. This is certainly an approximation, because some work would be needed to separate any asperities which had become welded to the other sphere. Further we ignore the effects of the roughness up to the point of contact. Now the flow tries to bring the particles together in the compressive quadrants of the shear $xy < 0$ and tries to separate them in the extensional quadrants $xy > 0$. Thus our model of the effect of the roughness is to replace the mobility function for motion along the line of centres with
$$A = 1 \quad \text{when both} \quad xy < 0 \quad \text{and} \quad r = 2 + \epsilon .$$
Otherwise we use the mobility functions given in the previous section.

The above model of roughness changes neither the tangential motion nor the rotational motion. For two close spheres, the resulting relative motion of the surfaces is small, and so possibly unimportant. Now it is possible to adopt an alternative simple model of the roughness. One can argue that the asperities fuse the particles and so the two spheres become locked and rotate as a single rigid body. Alternatively one can argue that the asperities act as gear teeth and the two particles roll around one another without slipping. By the antisymmetry of the flow, this no-slipping assumption also leads to the two spheres rotating together as a single solid body (in the case of spheres of equal size). To prevent the slipping, a tangential force and a torque are exchanged in addition to a normal force, and this modifies the mobility function $B(r)$. Now Wakiya (1971) and Nir & Acrivos (1973) have studied the rotation in a shear flow of two touching spheres which are locked together. Their analysis gave $B = 0.405$, which is the value obtained from our lubrication formula in the touching limit. For this alternative model of the effect of roughness, we set

$$A = 1 \quad \text{and} \quad B = 0.4046 \quad \text{when both} \quad xy < 0 \quad \text{and} \quad r = 2 + \epsilon.$$

These two models of the effect of the roughness represent two simple extremes. In a study of a heavy rough sphere sedimenting past a neutrally buoyant sphere, Davis (1992) found that the motion could be described by a solid friction model which lies between the two extremes which we have adopted. Smart, Beimfohr & Leighton (1993) found similarly for a rough particle slipping down an inclined smooth wall.

For near equatorial collisions, z small, the exact modelling of the effect of the roughness on the rotation is irrelevant. To calculate the final streamline, we need only the separation and orientation at the start of the extensional quadrant, i.e. $r = 2 + \epsilon$ and z when $x = 0$. Alternative models of the roughness may make the individual particles rotate differently while they are in contact in the compressional quadrant, but they do not change the separation $r = 2 + \epsilon$ and do not change much the orientation of the pair if $z \approx 0$ at the start of the extensional quadrant $x = 0$. Off the equatorial plane there may be some small differences between the orientation z when $x = 0$, but these differences must vanish both when $z = 0$ and when $y = 0$.

2.4. *Numerical results*

The governing equations for the trajectories of the pair of particles were integrated numerically using a fourth-order Runge–Kutta scheme. The time-step can be larger in the far field $r > 2.5$, where we took $\delta t = 0.01$. In the intermediate region $2.01 < r < 2.5$ we reduced the time-step to $\delta t = 0.005$. In the lubrication region $2 < r < 2.01$, the time-step was reduced further to $\delta t = 0.001$ to ensure that the radial separation changed little in one step. The errors in the numerical integration were then less than 10^{-3}. One test of the integration scheme is that it was able to reproduce the periodic closed doublet starting from $x = -3$, $y = 0.1$ and $z = 0.1$ without noticeable change of the amplitude over more than 5 cycles. Of course for the migration across streamlines, we are only interested in the open trajectories in which the particles start and terminate infinitely far apart.

Figure 1 shows some typical trajectories of one sphere relative to the other in the (x, y)- and (x, z)-planes. With no surface roughness $\epsilon = 0$, the trajectory is symmetric; the spheres return to their initial streamlines after the collision. For the trajectory starting at $x = -10$ and $y = z = 0.1$, the minimum separation of the smooth spheres is 4.75×10^{-5}. Figure 1 shows that the collisions become asymmetrical once the surface roughness ϵ is greater than this minimum separation: the spheres now separate on streamlines further apart than on their approach. Because the trajectories crowd
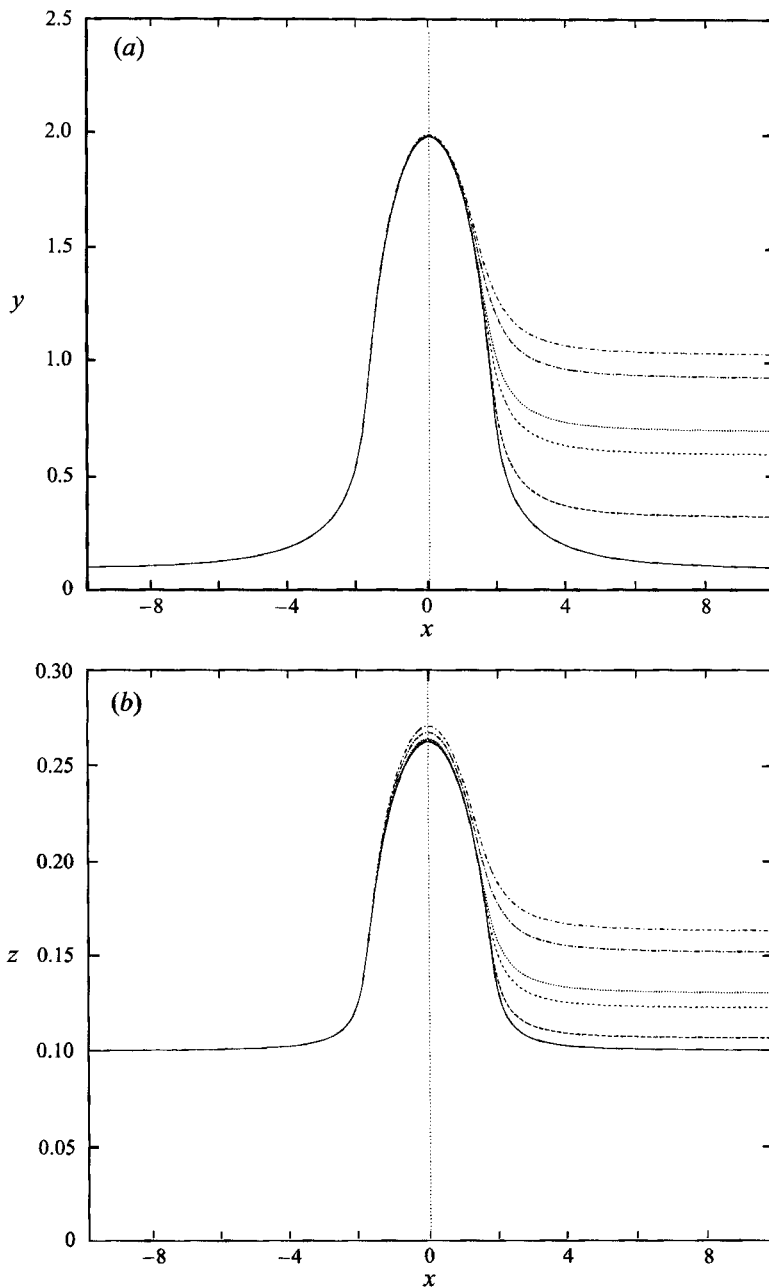
FIGURE 1. The effect of roughness on particle trajectories, (a) in the (x, y)-plane and (b) in the (x, z)-plane. The initial conditions are $x = -10$ and $y = z = 0.1$. The different curves correspond to different values of the roughness: ————, $\epsilon = 0$; — — — — —, $\epsilon = 10^{-4}$; — — — — —, $\epsilon = 5 \times 10^{-4}$; ----------, $\epsilon = 10^{-3}$; — · — · — · —, $\epsilon = 5 \times 10^{-3}$ and — · · — · · — · ·, $\epsilon = 10^{-2}$.

considerably during the collision, quite a small displacement by the roughness across the crowded trajectories produces a large displacement across the final streamlines.

It is useful to estimate the scaling of this crowding of the trajectories. Batchelor & Green (1972*b*) showed that in a general linear shearing flow the probability density function is only a function of the scalar distance between the two non-Brownian spheres, so long as the particles start at a great separation with a uniform probability density function. They derive the probability density function

$$p(r) \; = \; \frac{n}{1-A} \exp \int_r^\infty \frac{3(B-A)}{r(1-A)} \, \mathrm{d}r \; .$$

Using our mobility functions A and B, which are based on more accurate calculations than those available to Batchelor & Green, we find that in the lubrication region

$$p \; \sim \; nk\xi^{-0.7813} \, (L+1.347)^{-0.3506} \; ,$$

where $\xi = r - 2$ and $L = \ln(1/\xi)$. Now when the spheres are aligned perpendicular to the flow, they move around one another with an $O(\gamma)$ velocity. Hence in this orientation the flux of trajectories with $2 < r < 2 + \epsilon$ and $|z| < 1$ is $n\gamma k'\epsilon^{0.2187} \left(\ln(1/\epsilon) + 1.347 \right)^{-0.3506}$, assuming that ϵ is much larger than the minimum separation of the open trajectories. Now when the spheres are greatly separated, they move apart with velocity γy. Hence in the far field the flux of trajectories with $0 < y < \delta$ and $|z| < 1$ is $\frac{1}{2}n\gamma\delta^2$. Equating these two fluxes, we find that trajectories with separation $\delta(\epsilon) = O\left(\epsilon^{0.1093} \left(\ln(1/\epsilon) + 1.347\right)^{-0.1753}\right)$ crowd together to an ϵ separation as the spheres pass.

2.5. Displacements across streamlines

To calculate the shear-induced dispersion, we are interested in the net displacement across streamlines caused by a collision. Numerical computations follow the trajectory $x(t)$ starting the spheres at a great separation on approaching streamlines, $x \rightarrow -\infty$ with $y^{-\infty} > 0$, and integrating until the spheres are again at large separations, now on the receding streamline $x \rightarrow \infty$. Using the centre of mass motion given earlier, we find that the net streamline displacement of the first sphere is

$$\Delta X_2 \; = \; X_2^{+\infty} - X_2^{-\infty} \; = \; \tfrac{1}{2} \left(y^{+\infty} - y^{-\infty} \right) \; ,$$

and similarly

$$\Delta X_3 \; = \; \tfrac{1}{2} \left(z^{+\infty} - z^{-\infty} \right) \; .$$

To avoid computations to very large separations, which take a long time on the slow trajectories with y small, we use two extrapolations from a more moderate value of the separation, $x = \pm 10$. In the case of fast trajectories, when $x \gg 1$ and y and z are $O(1)$, the first approximation to the trajectory is a straight line $x \sim x_0 + y_0 t$, $y \sim y_0$ and $z \sim z_0$. At the next approximation

$$\dot{y} \; \sim \; -\frac{(5y_0^2 + \tfrac{8}{3})(x_0 + y_0 t)}{\left[(x_0 + y_0 t)^2 + y_0^2 + z_0^2\right]^{5/2}} \quad \text{and} \quad \dot{z} \; \sim \; -\frac{5(x_0 + y_0 t)}{\left[(x_0 + y_0 t)^2 + y_0^2 + z_0^2\right]^{5/2}} \; .$$

Integrating we find

$$y^\infty \; \sim \; y + \frac{\dot{y}r^2}{3\dot{x}x} \quad \text{and} \quad z^\infty \; \sim \; z + \frac{\dot{z}r^2}{3\dot{x}x} \; .$$

In the case of slow trajectories, when $x \gg 1$, $y \ll 1$ and $z = O(1)$, the governing
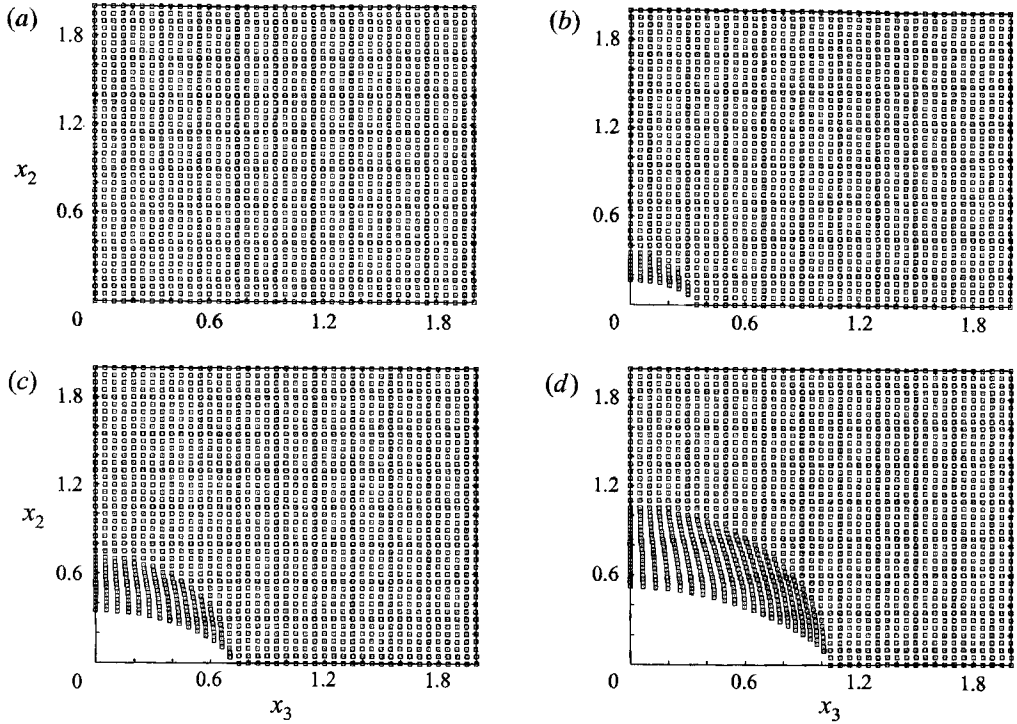
FIGURE 2. Distributions of final streamlines $(X_2^{+\infty}, X_3^{+\infty})$ for the first sphere which started with $(X_2^{-\infty}, X_3^{-\infty})$ on a regular grid on $[0,2] \times [0,2]$. The second sphere starts at the origin, $Y^{-\infty} = 0$. The different panels correspond to different values of the roughness: (*a*) $\epsilon = 3 \times 10^{-5}$, (*b*) $\epsilon = 10^{-4}$, (*c*) $\epsilon = 10^{-3}$, (*d*) $\epsilon = 10^{-2}$.

equations reduce to

$$\dot{x} \sim y, \qquad \dot{y} \sim -\tfrac{8}{3}x(x^2 + z^2)^{-5/2} \qquad \text{and} \qquad \dot{z} \sim 0.$$

Integrating we find

$$y^\infty \sim \left(y^2 - \tfrac{16}{9}(x^2 + z^2)^{3/2}\right)^{1/2} \qquad \text{and} \qquad z^\infty \sim z.$$

These two extrapolations agree when $y - y^\infty \ll y \ll 1$. For $x = \pm 10$, a convenient cross-over is at $y = 0.1$. Applying the extrapolation, the eventual streamline position is found with an error of less than 10^{-3}.

To represent the net streamline displacements, we plot in figure 2 the final coordinates $(X_2^{+\infty}, X_3^{+\infty})$ of the first sphere which started on a regular grid in $0 \leqslant X_2^{-\infty} \leqslant 2$, $0 \leqslant X_3^{-\infty} \leqslant 2$; the second sphere starts at the origin, $Y^{-\infty} = 0$. The pictures would be reproduced in $X_3^{+\infty} < 0$ symmetrically about the axis $X_3^{+\infty} = 0$. Note that for the convenience of the later calculation of the diffusivities we use coordinates in which the second sphere starts at the origin rather than the more usual coordinates in which the centre of mass of the two spheres is fixed at the origin.

For a surface roughness $\epsilon = 3 \times 10^{-5}$, smaller than the minimum separation of the open trajectories of smooth spheres, all the trajectories return to their original streamlines, i.e. the original regular grid in figure 2(*a*), and there is no net displacement. With increasing roughness there are progressively larger displacements of the streamlines. We note that the displacements are mainly in the X_2-direction, the direc-

tion of the velocity gradient, although there is some displacement in the X_3-direction, the direction of the vorticity.

In figure 2 we see that the surface roughness produces an excluded region with no final trajectories and a region where the trajectories are compressed outwards. This structure has a simple form for planar collisions, with $z = 0$. Consider the trajectory which has a separation equal to the surface roughness $r = 2 + \epsilon$ when the particles are perpendicular to the flow, $x = 0$. Let δ be the value of the final height y^{∞} for this trajectory. By symmetry all trajectories with initial heights $0 < y^{-\infty} < \delta$ must have their spheres coming into contact through surface roughness in the compressional quadrant $x < 0$. These spheres then move around one another at the separation $r = 2 + \epsilon$ until perpendicular to the flow, when they separate on the single half-trajectory with $y^{+\infty} = \delta$. For these trajectories the streamline displacement is $\Delta X_2 = \frac{1}{2}(\delta - X_2^{-\infty})$ for $0 < X_2^{-\infty} \leqslant \delta$, i.e. in figure 2 there is an excluded region $0 < X_2^{+\infty} < \frac{1}{2}\delta$ and a linearly compressed region $\frac{1}{2}\delta \leqslant X_2^{+\infty} \leqslant \delta$. Figure 2 shows that there is a very similar behaviour for non-planar collisions, $z \neq 0$, slightly distorted by the displacements in the vorticity z-direction.

3. Dispersion coefficients

3.1. *Self-diffusion*

In self-diffusion, a single marked particle executes a random walk in a suspension at a uniform concentration. The self-diffusivity is half the rate of change in time of the variance of the displacement of the random walk. In this paper the random walk is across the streamlines and is due to collisions with other particles in the shear flow. We will calculate the diffusivities for displacements in the y-direction and in the z-direction.

We consider a dilute suspension with a uniform concentration. Let n be the number density of the particles in the suspension and so the volume fraction is $\phi = n\frac{4}{3}\pi a^3 \ll 1$. We assume that there are no long-range correlations in the suspension, so that the probability distribution of particles which collide with a test sphere is uniform in space when they are far upstream. Hence the rate of collisions with relative displacements in $(y^{-\infty}, y^{-\infty} + \delta y^{-\infty}) \times (z^{-\infty}, z^{-\infty} + \delta z^{-\infty})$, which have spheres approaching at a velocity $\gamma|y^{-\infty}|$, is $n\gamma|y^{-\infty}|\delta y^{-\infty}\delta z^{-\infty}$. A collision with these parameters produces a net displacement of the test sphere $(-\Delta X_2, -\Delta X_3)$ with $\Delta X_i(y^{-\infty}, z^{-\infty}, \epsilon)$. Since we are assuming that each of these collisions is uncorrelated, we have self-diffusivities

$$D_i^s = \frac{1}{2} \int_{-\infty}^{\infty} \int_{-\infty}^{\infty} (\Delta X_i)^2 n\gamma|y^{-\infty}| \, dy^{-\infty} dz^{-\infty} \qquad (i = 2 \text{ or } 3).$$

Non-dimensionalizing the lengths in the integral with the radius of the sphere a, we have

$$D_i^s = \phi a^2 \gamma \frac{3}{8\pi} \int_{-\infty}^{\infty} \int_{-\infty}^{\infty} (\Delta X_i)^2 |y^{-\infty}| \, dy^{-\infty} dz^{-\infty} \qquad (i = 2 \text{ or } 3).$$

The above integral was evaluated numerically over the grid of $y^{-\infty}z^{-\infty}$-points shown in figure 2 using a trapezoidal rule. The spacing of 0.05 between points produced an error less than 0.1%. By symmetry we integrated over the positive quadrant and quadrupled the answer. Further there is no need to extend the range of integration outside the square of length 2 for the values of surface roughness considered, because the integrand vanished identically well inside this square.

Figure 3 gives the results for the self-diffusivities for roughness from 10^{-3} to 8×10^{-2}.
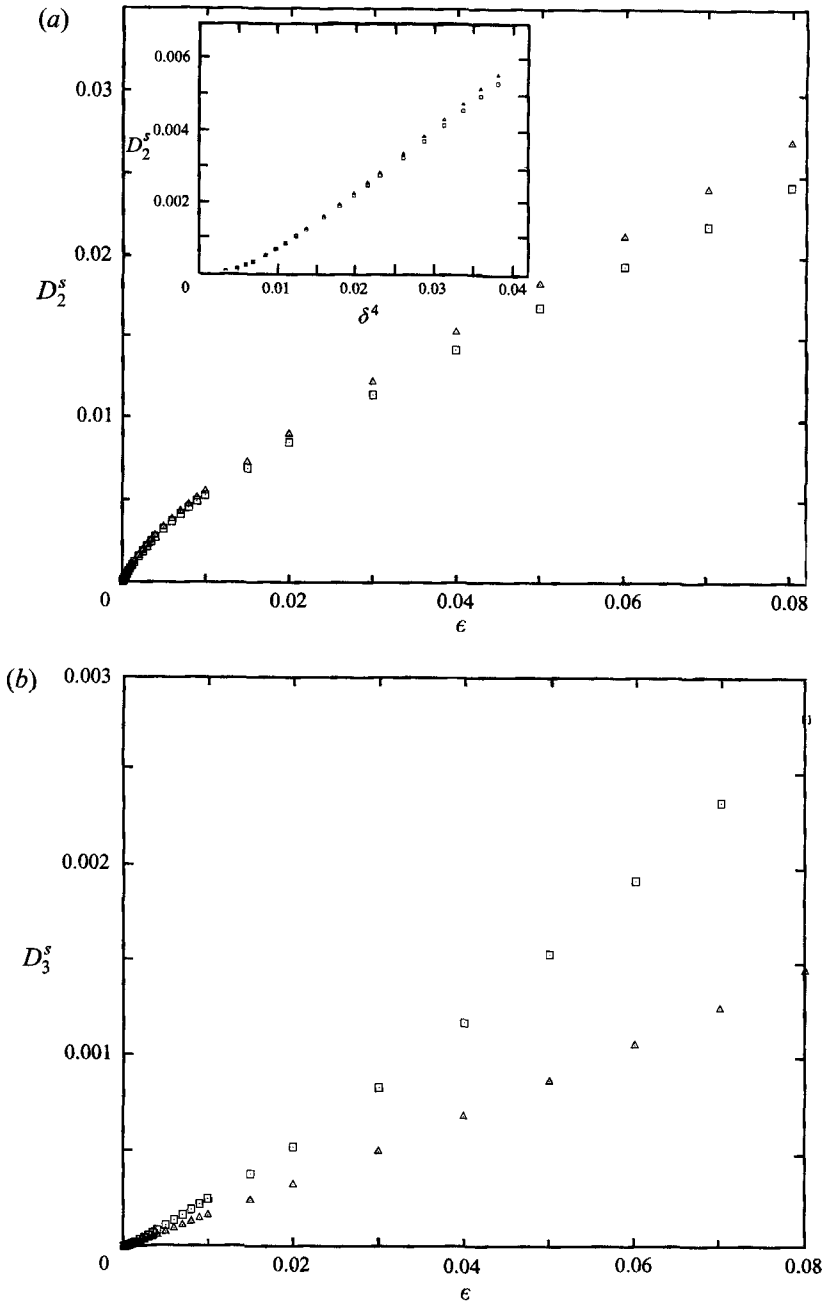
FIGURE 3. The self-diffusivities divided by $\phi a^2 \gamma$ as a function of the surface roughness: (a) for diffusion in the direction of the gradient of velocity, and (b) for diffusion in the direction of the vorticity. Results for the model of surface roughness with only a normal force are given by the points □, and for the alternative model with the two spheres locked together by the points △. In the insert the diffusivity has been plotted against the scaling $\delta^4(\epsilon) = \epsilon^{0.4374} \left(\ln(1/\epsilon) + 1.347 \right)^{-0.7012}$

From the vertical scales of the figure, we note that the diffusion is very anisotropic, with the diffusivity in the direction of the vorticity being less than 10% of that in the direction of the velocity gradient, much less than 10% at small surface roughnesses. Guided by the earlier discussion of the large $\delta(\epsilon)$ displacements in the final streamline caused by a small surface roughness ϵ, we found that the diffusivity D_2^s in the gradient direction is approximately linear in $\delta^4(\epsilon) = \epsilon^{0.4374} \left(\ln(1/\epsilon) + 1.347\right)^{-0.7012}$ over the range $10^{-4} \leqslant \epsilon \leqslant 10^{-3}$, see insert to figure 3. The magnification of the insert also shows that there is a minimum roughness, equivalent to the minimum separation of the open trajectories, below which the diffusivity vanishes. The diffusivity D_3^s in the vorticity direction seems to be approximately linear in ϵ in the range plotted.

The two different models of the effect of surface roughness produce very similar results. The first model with just a normal force in the compressional quadrant produces a slightly smaller diffusivity in the direction of the velocity gradient. The second model with the two spheres rotating as a single fused body has a lower diffusivity in the direction of the vorticity, roughly half the value from the first model.

Now in recent experiments Biemfohr et al. (1993) found self-diffusivities of $2.3 \times 10^{-2}\phi a^2\gamma$ in the dilute limit. We note that for the surface roughness of $\epsilon = 0.02$ our D_2^s is $8 \times 10^{-3}\phi a^2\gamma$, i.e. a non-negligible contribution while not fully explaining the observations. Biemfohr et al. suggest that the non-sphericity of their particles with an aspect ratio of about 1.19 made an important contribution to the dispersion. Indeed if we view this non-sphericity as a gross roughness of $\epsilon = 0.09$, then we do predict the measured self-diffusivity. Future studies should investigate the interaction between two smooth spheroidal particles.

3.2. Down-gradient diffusion

We now consider a suspension which has a small gradient in the concentration in a direction across the streamlines, separately in the direction of the velocity gradient and in the direction of the vorticity, i.e.

$$n(\mathbf{x}) = n_0 + x_i \frac{\partial n}{\partial x_i} \qquad (i = 2 \text{ or } 3).$$

We need to calculate the rate at which particles cross unit area of a plane perpendicular to the concentration gradient, $x_i = 0$ for $i = 2$ or 3, due to displacements across the streamlines.

Consider a test sphere starting at $X^{-\infty}$ being displaced $\Delta X = X^{+\infty} - X^{-\infty}$ across the streamlines as a result of a collision with a second sphere starting at $Y^{-\infty}$. With the relative separation (x, y, z) of the two spheres, $x = X - Y$, the rate of these collisions is $n(Y^{-\infty})\gamma|y^{-\infty}|$. For a given initial separation of the colliding pair $x^{-\infty}$, and hence given final displacement across the streamlines ΔX, any test sphere starting with $X_i^{-\infty}$ in the range $-\Delta X_i < X_i^{-\infty} < 0$ will cross the plane perpendicular to the concentration gradient, $x_i = 0$, from the negative side. There is a smilar range on the positive side when $\Delta X_i < 0$. Hence the net flux of particles across the plane is

$$\int_{-\infty}^{\infty} \int_{-\infty}^{\infty} \left[\int_{-\Delta X_i}^{0} n(X_i^{-\infty})n(Y_i^{-\infty})\gamma|y^{-\infty}|\,\mathrm{d}X_i^{-\infty} \right] \mathrm{d}y^{-\infty}\mathrm{d}z^{-\infty} \qquad (i = 2 \text{ or } 3)$$

taking into account both cases $\Delta X_i >$ and < 0. We substitute $Y_i^{-\infty} = X_i^{-\infty} - x_i^{-\infty}$ and substitute the linear variation of the concentration neglecting terms quadratic in the
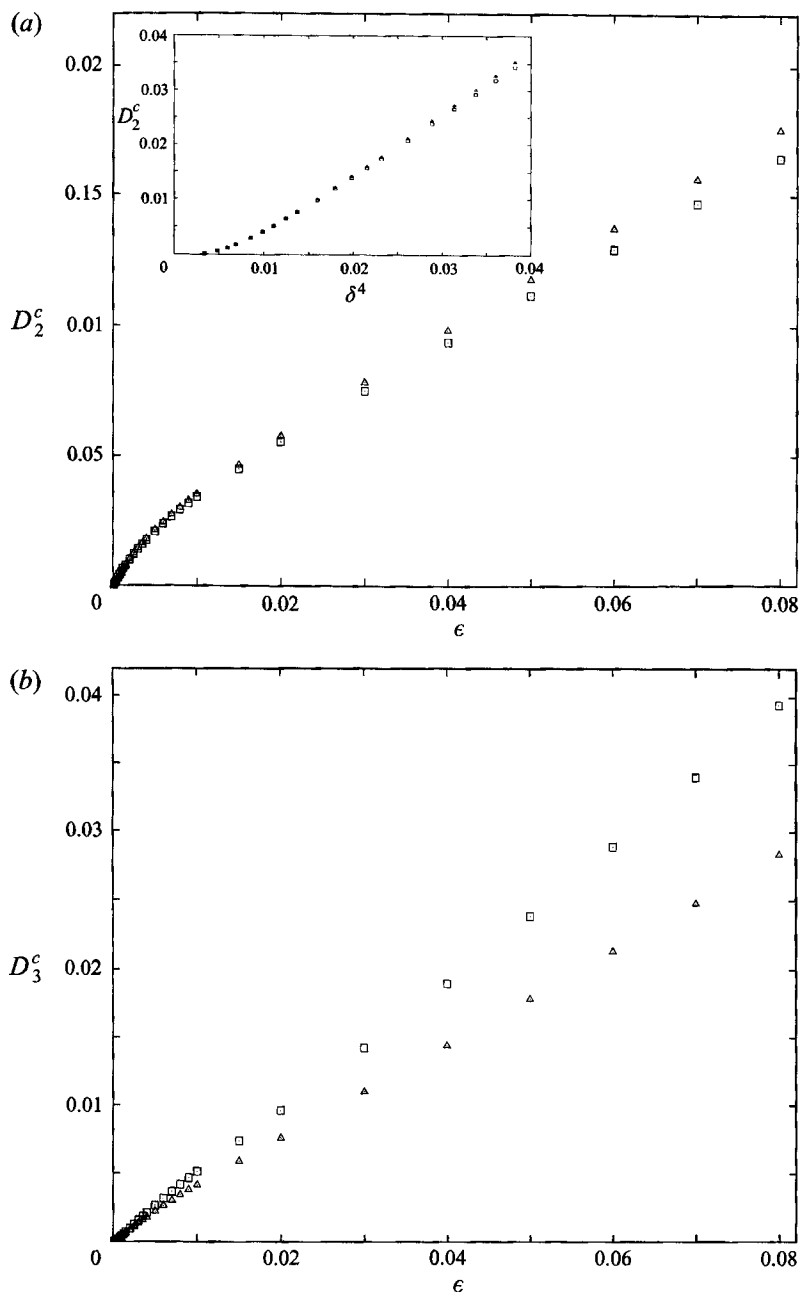
FIGURE 4. Down-gradient diffusivities. See caption to figure 3 for details.

gradient. Then integrating, we find a flux equal to

$$\int_{-\infty}^{\infty}\int_{-\infty}^{\infty}\left[n_0^2 \Delta X_i - n_0\frac{\partial n}{\partial x_i}\left(-\Delta X_i^2 - x_i^{-\infty}\Delta X_i\right)\right]\gamma|y^{-\infty}|\,\mathrm{d}y^{-\infty}\mathrm{d}z^{-\infty}\qquad (i = 2 \text{ or } 3).$$

The first term in the square bracket vanishes, as averaging over the collisions there is no net displacement. Hence the flux is proportional to the concentration gradient, with the coefficient of proportionality being a diffusivity. Non-dimensionalizing the

lengths in the integrand with a, we have the diffusivities

$$D_i^c = 2D_i^s + \phi a^2 \gamma \frac{3}{4\pi} \int_{-\infty}^{\infty} \int_{-\infty}^{\infty} x_i^{-\infty} \Delta X_i |y^{-\infty}| \, dy^{-\infty} dz^{-\infty} \qquad (i = 2 \text{ or } 3).$$

One of the two D_i^s is the standard contribution of the random walk to a flux down a concentration gradient. The other D_i^s, together with the final integral, is due to the slightly higher concentration of particles colliding on one side of a test sphere systematically nudging it across the streamlines towards the lower concentration.

This integral was evaluated as for the self-diffusivities. Figure 4 gives the results for surface roughnesses from 10^{-3} to 8×10^{-2}. We first note that the diffusivities for self-diffusion differ from those for down-gradient diffusion, because interactions between the particles are essential for both dispersions. In the dilute limit of $\phi = 0$, the diffusivities are equal, with common value 0. We find that the down-gradient diffusivities are larger than the self-diffusivities by a factor of 6 for the direction of the velocity gradient and by a factor of 12 for the direction of the vorticity. As a consequence, the diffusivities are less anisotropic for down-gradient diffusion compared with self-diffusion. The results for the two models of the effect of surface roughness are again similar. We have no experimental results with which to compare our predictions.

REFERENCES

ACRIVOS, A., BATCHELOR, G. K., HINCH, E. J., KOCH, D. L. & MAURI, R. 1992 Longitudinal shear-induced diffusion of spheres in a dilute suspension. *J. Fluid Mech.* **240**, 651–657.

ARP, P. A. & MASON, S. G. 1977 The kinetics of flowing dispersions. IX. Doublets of rigid spheres. *J. Colloidal Interface Sci.* **61**, 44–61.

BATCHELOR, G. K. & GREEN, J. T. 1972a The hydrodynamic interaction of two small freely-moving spheres in a linear flow field. *J. Fluid Mech.* **56**, 375–400.

BATCHELOR, G. K. & GREEN, J. T. 1972b The determination of the bulk stress in a suspension of spherical particles to order c^2. *J. Fluid Mech.* **56**, 401–427.

BIEMFOHR, S., LOOBY, T., BIEMFOHR, S. & LEIGHTON, D. T. 1993 Measurement of shear-induced coefficient of self-diffusion in dilute suspensions. In the *Proc. DOE/NSF Workshop on Flow of Particles and Fluids, Ithaca, NY.*

BOSSIS, G. & BRADY, J. F. 1987 Self-diffusion of Brownian particles in concentrated suspensions under shear. *J. Chem. Phys.* **87**, 5437–5448.

DAVIS, R. H. 1992 Effects of surface roughness on a sphere sedimenting through a dilute suspension of neutrally buoyant spheres. *Phys. Fluids* A **4**, 2607–2619.

ECKSTEIN, E. C., BAILEY, D. G. & SHAPIRO, A. H. 1977 Self-diffusion of particles in shear flow of a suspension. *J. Fluid Mech.* **79**, 191–208.

KIM, S. & KARRILA, S. J. 1991 *Microhydrodynamics: Principles and Selected Applications.* Butterworth-Heinemann.

LEIGHTON, D. T. & ACRIVOS, A. 1987a The shear-induced migration of particles in concentrated suspensions. *J. Fluid Mech.* **181**, 415–439.

LEIGHTON, D. T. & ACRIVOS, A. 1987b Measurement of shear-induced self-diffusion in concentrated suspensions of spheres. *J. Fluid Mech.* **177**, 109–131.

LIN, C. J., LEE, K. J. & SATHER, N. F. 1970 Slow motion of two spheres in a shear flow. *J. Fluid Mech.* **43**, 35–47.

NIR, A. & ACRIVOS, A. 1973 On the creeping motion of two arbitrary-sized touching spheres in a linear shear field. *J. Fluid Mech.* **59**, 209–223.

SMART, J. R., BEIMFOHR, S. & LEIGHTON, D. T. 1993 Measurement of translational and rotational velocities of a non-colloidal sphere rolling down a smooth inclined plane at low Reynolds number. *Phys. Fluids* A **5**, 13–24.

SMART, J. R. & LEIGHTON, D. T. 1989 The measurement of the hydrodynamics surface roughness of non-colloidal spheres. *Phys. Fluids* A **1**, 52–60.

WAKIYA, S. 1971 Slow motion in shear flow of a doublet of two spheres in contact. *J. Phys. Soc. Japan* **31**, 1581–1587.

WANG, Y., MAURI, R. & ACRIVOS, A. 1995 Transverse shear-induced diffusion of spheres in a dilute suspension. *J. Fluid Mech.* (submitted)